Invited Paper

Propagation of terahertz waves in one-dimensional metallic wire arrays

Hui Feng [1, 2] and Li Wang [1*]
[1] Beijing National Laboratory for Condensed Matter Physics, Institute of Physics, Chinese Academy of Sciences, Beijing 100190, China
[2] Research Center for Microwave Photonics, East China Research Institute of Electronic Engineering, Hefei 230088, China
[*1] Email: wangli@aphy.iphy.ac.cn

(Received January 2, 2013)

Abstract: Experiment and simulation of the guiding of terahertz electromagnetic wave in one dimensional metallic wire arrays are performed. Our wire array structure supports two propagating modes with frequencies c/d and $c/2d$, where c is the speed of light in vacuum and d is the distance between the two adjacent wires. The attenuations of the two modes are 0.16 dB/wire and 0.71 $dB/wire$, respectively.

Keyword: Terahertz, Propagation, Metallic wire array, Subwavelength, Resonance

doi: 10.11906/TST.059-065.2013.03.04

After the idea of a subwavelength-sized waveguide represented by a linear chain of spherical metal nanoparticles, in which light was transmitted by electrodynamic interparticle coupling, was proposed by M. Quinten *et al* [1], the guided wave propagating in this kind of system has received extensive attention because the light can be effectively confined to something with the dimensions much smaller than the diffraction limit during propagation. J. R. Krenn *et al* reported the experimental observation of near-field optical effects close to Au nanoparticles using a photon scanning tunneling microscope [2]. Stefan A. Maier *et al* presented observations of electromagnetic energy transport from a localized subwavelength source to a localized detector over a distance of about 0.5 μm in plasmon waveguides consisting of closely spaced silver rods [3]. The electromagnetic energy transport along array of closely spaced metal rods as an analogue to plasmonic devices was also reported in microwave frequencies [4]. Due to the unique properties of the terahertz radiation, metal wire was widely used to manipulate the electromagnetic wave in this frequency range. J. B. Pendry *et al* have demonstrated that a very simple metallic microstructure comprising a regular array of thin wires exhibits novel electromagnetic properties in GHz region [5]. Even a bare metal wire can be used to transport terahertz pulse [6]. G. Shvets *et al* reported the imaging, magnification and radiation focusing in the subwavelength spatial scale using tapered arrays of thin metallic wires [7]. In a previous publication, we calculated the extinction spectra for 1-D chains of subwavelength-sized metal spheres responding to incident terahertz plane waves in 0.1-2.5 *THz* frequency range using a generalized Mie theory. It is found that the coherent coupling between the spheres varies as the number of spheres in the ensemble increases and finally approaches a steady response, which manifests that the collective excitation of the spheres only exists within a finite spatial scope [8]. In this paper, we report the experimental observation and simulation of guided THz pulses in one-dimensional metallic wire arrays. Our results show that this system has low dispersion and reasonable transmitting efficiency.

Our experiment was conducted by a modified terahertz time-domain spectrometer (THz-TDS) shown in Fig.1. A femtosecond laser beam with a 70 *fs* pulse duration at 800 *nm* and a repetition rate of 80 *MHz* from a mode-locked Ti: Sapphire laser (Mai Tai, Spectra Physics) was split into two beams by a beam splitter. One was for generating THz radiation in a <110> cut ZnTe wafer by optical rectification [9], and the other was for detecting THz wave in a <110> cut ZnTe wafer by EO sampling [10]. The whole terahertz wave path was enclosed in a vacuum chamber to prevent the absorption of water vapor. The inset of Fig.1 shows the structure of the metallic wire arrays. The copper wires with a radius *r* lay in the XZ plane and parallel to the Z axis, and the distance between the two adjacent wires was *d*. The wire array lined along X axis. The wire marked No.1 was placed in the focus of the paraboloidal mirror P3. The incident terahertz pulses polarized along the X axis was focused onto the *n*th wire by the off-axis paraboloidal mirror P2. The terahertz pulse propagated along the wire arrays was collected, collimated and focused to the detector by off-axis paraboloidal mirrors P3 and P4. The THz spot diameter at the focal point of P2 was approximately 2 *mm*, so there were five wires with indices from *n-2* to *n+2* were illuminated by incident terahertz waves for samples used. The paraboloidal mirror P2 was mounted on a linear translation stage which can move along the X axis so that the travel distance of THz pulses across the array can be changed by moving the stage while the whole geometric beam path length keeps the same.

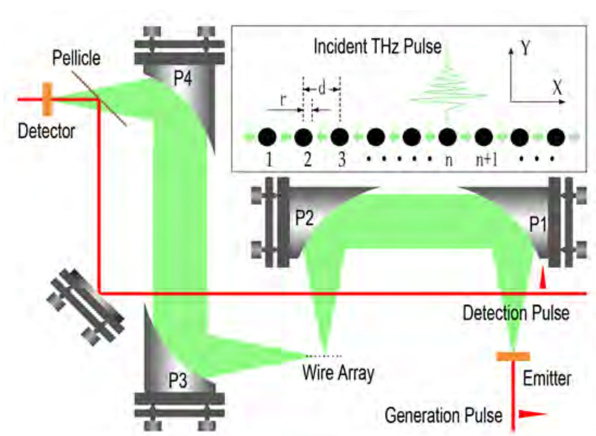

Fig. 1 Experiment setup. P1-P4 are off-axis paraboloidal mirrors. The incident terahertz beam is focused onto the *n*th wire by P2. The inset shows our metal wire array structure: the radius of the wire is *r* and the distance between the two adjacent wires is *d*.

For the experiment configuration described above, the charge oscillation and associated electromagnetic(EM) fields in metallic wires induced by incident THz waves have two orthogonal components, which are along X and Y axis, respectively. It is clear that only the Y direction polarized field can be collected by P3. Fig. 2(a) shows the measured temporal waveforms of the incident terahertz pulse and the THz pulse re-emitted from the wire arrays with *r*=90 μm, *d*=360 μm and *n*=7 (the position of the incident THz spot). Analogous to transmission spectrum in conventional THz-TDS, which is the ratio of the transmitted electric field to the incident electric field in the frequency domain, we utilize the ratio of the electric field after passing the wire arrays to the incident electric field to analyze the propagation properties of the terahertz pulse in the wire arrays. In the following, we will call the ratio *propagation spectrum* for convenience. Fig. 2(b) shows the propagation spectrum of the terahertz pulses plotted in Fig. 2(a). It can be seen that there are two propagating modes at 0.8 *THz* and 1.59 *THz*. The propagation spectrum calculated by two-dimensional finite-difference time-domain (FDTD) simulation is also shown in Fig. 2(b). The experiment results and the FDTD simulation agree well. Because the signal to noise ratio of our experiment results is low, we use FDTD simulation results to discuss the THz wave propagation in the following sections.

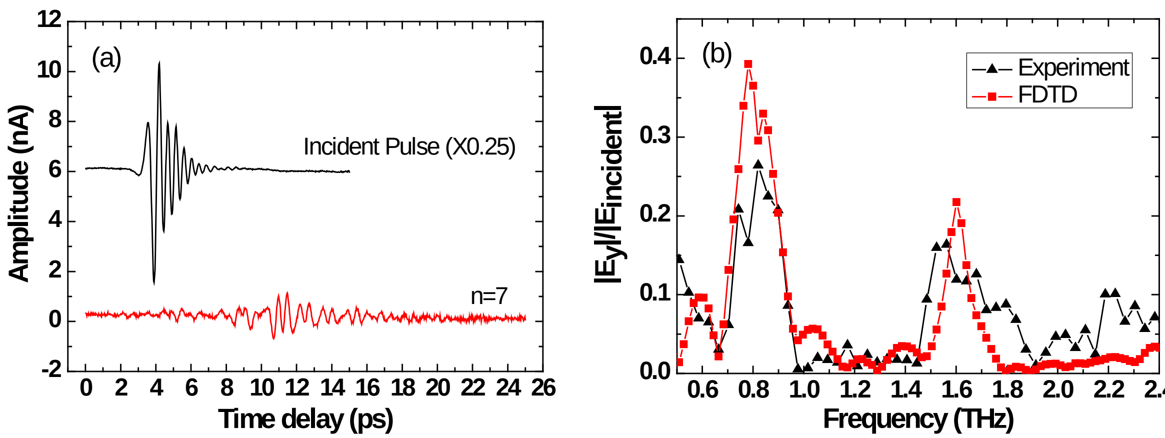

Fig. 2 (a) Temporal waveform of the incident THz pulse and that passing the wire array with the incident position *n*=7. The waveform of the incident pulse is shifted and rescaled for the convenience of comparison. (b) The propagation spectra of experiment measurement and FDTD simulation.

It is noticeable in Fig. 2(b) that there is a split in the first resonant peak at approximately 0.8 *THz*. In order to figure out the origin of the split, we simulated the terahertz pulses propagating along two wire arrays with different total wire numbers, but keep the incident position the same, i.e, incident onto the same *n*th wire. Fig. 3(a) shows the incident pulse used in our simulation and two pulses after propagating along the arrays with incident on *n*=7 in both arrays. The terahertz pulse passing the array with 25 wires oscillates much more cycles after the main pulse than that with 9 wires. This phenomenon can be understand by considering the interference effect: when the terahertz pulse incident onto the array, the first 5 wires are excited and the charge oscillations induce the retarded oscillations in the neighboring wires of both sides, which forms near field excitations propagating along both positive X and negative X directions.

Considering the pulse propagating along positive X direction, the arrays have different wire numbers will produce different backward propagating components, including the strong back-scattered waves from the end of the array. Therefore, the array length dependent interference takes into effect. Fig. 3(b) shows the propagation spectra of both wire arrays, there is a split on the first peak of the propagation spectrum for the arrays with 25 wires, and disappeared for the arrays with 9 wires. This is because when the total wire number is 9 and the THz pulse is focused onto the 7th wire, the 5th to 9th wires are illuminated by the THz pulse. The induced field propagating to only one side of the wire array and no interference is observed.

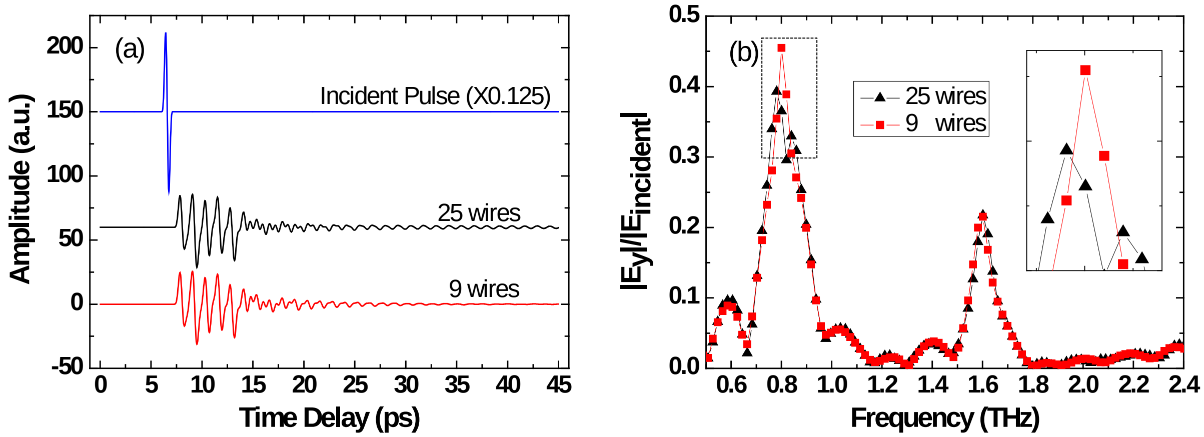

Fig. 3 (a) Temporal waveform of incident pulse and re-emitted pulses after passing the wire array with the incident position *n*=7 while the total wire number is different. The waveform of the incident pulse and the pulse after propagating along array with 25 wires are shifted, and the incident pulse is also rescaled. (b) Propagation spectra of the pulses show in (a). The inset shows an enlarged view around the first peak.

In the following, we will focus our attention to analyze the propagation properties of the terahertz pulse in the one-dimensional metal wire arrays, including speed, attenuation and resonant mode frequencies. First, we calculated the speed by simulating the terahertz pulse propagated along arrays with different incident position, the *n*th wire, while kept the total wire number equal to *n*+2. So the pulse only propagated to one side of the array, which avoided the unwanted interference. We choose $r=90\,\mu m$ and $d=4r$ in all the arrays with different wire numbers Fig. 4(a) shows the temporal waveforms for different *n*. The shape of the waveforms are all similar, which means that the dispersion is small, and the major difference is the amplitude getting smaller for longer travel distance in the arrays. We can also conform this from Fig. 4(b), which shows the normalized spectra of the terahertz pulses shown in Fig. 4(a). Considering the low dispersion property of the terahertz pulse propagated along the arrays, we chose the first positive peak in the temporal waveform as the arrival time marker of the pulse at the detector, and measured the distance between the *n*th wire and the detector as the path length of the THz pulse. Then we plotted the path length as a function of time shown in the inset of Fig. 4(a). The data in the inset is a linear fit and the slope of the line is 0.298 *mm/ps*, corresponding to a propagating speed along the wire arrays nearly equal to *c*, the speed of light in vacuum. We also calculated the speed of the terahertz pulse propagating along the wire array with *d*=3.2*r*. The speed is

0.28 *mm/ps*, also very close to *c*. This result is quite unexpected because the THz fields propagating in the arrays are mainly facilitated by charge-field coupling, which means frequent and strong energy exchange should happen during the process. The inset of Fig. 4(b) shows the attenuation of the two modes. The square and triangular dots represent the amplitude of the two modes as a function of incident position *n*, and the two curves are the exponential fit of the two sets of dots. The obtained attenuations of the two modes are 0.16 *dB/wire* and 0.71 *dB/wire*, respectively. The second mode decays much faster than the first one, therefore, the interference effect is much smaller. This is consistent with the observations that there is a split in the first propagation peak at 0.8 *THz* as shown in Fig. 2(b) while there is no split in the second propagation peak at 1.59 *THz*.

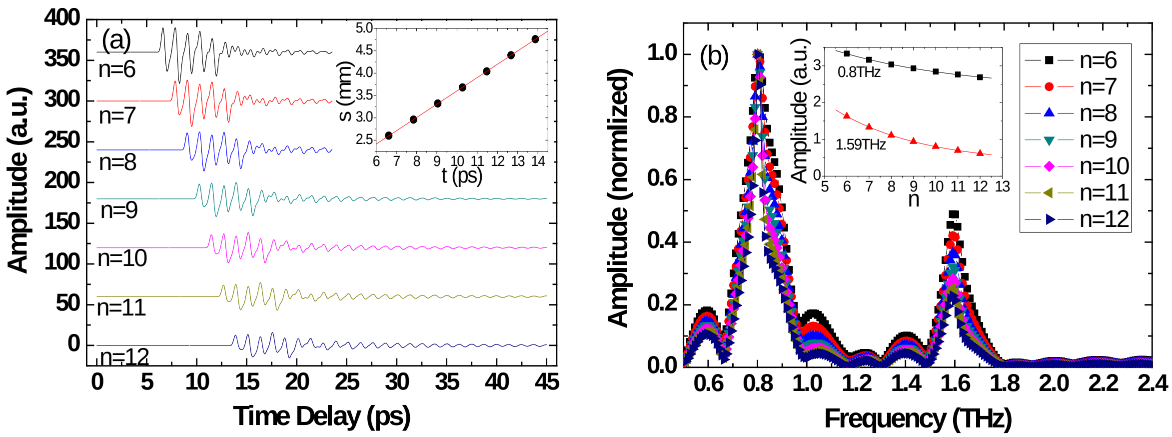

Fig. 4 The speed and attenuation of the THz wave travelling through the metal wires. (a)Temporal waveforms of the THz pulse passing the arrays with different wire numbers. The inset shows the path length in array as a function of time and the slope of the linear fitting gives the speed of THz waves. (b) Spectra normalized to the first peak. The inset shows the attenuations of the two modes at 0.8 *THz* and 1.59 *THz*.

Finally, we calculated the geometry dependent frequencies of the two modes supported by the wire arrays. We fixed the radius of the wires r=90 μm while changing the distance between the wires from d =3.4r to 4.2r with an increment of 0.2r. The terahertz pulse was focused onto the 9th wire and the arrays has 11 wires. Fig. 5 shows the propagation spectra of different array structures. In the inset we plot the frequencies of the two modes as a function of c/d. The two lines represent $f=c/d$ and $f=2c/d$, respectively. Our wire array structure can be considered as a grating. When a light wave with wavevector **k** incident on the surface, diffraction gives rise to a series of diffracted waves. The wavevector of the diffracted wave $\mathbf{k}_m$ is: $\mathbf{k}_m = \mathbf{k} + m\mathbf{G}$, where m is the diffraction order and **G** is the grating vector [11]. The grating vector lies in the plane of the grating and is perpendicular to the grooves. For the array structure considered here, it can be expressed as $\mathbf{G} = 2\pi / d\hat{x}$, where $\hat{x}$ is the unit vector in X direction. Because of the normal incidence of the THz waves, the components of the wavevector of the diffracted wave in the plane of the array are $\mathbf{k}_{xm} = m(2\pi / d)$. Depending on the spectra range of the incident terahertz pulse and the structure of the arrays, four modes with $m = \pm 1$ and $m = \pm 2$ can be generated. The energy of the diffracted wave can propagate along the wire array structure by inter-wire coupling. The two modes with *m*=1 and 2 propagate along positive X direction while the other two modes propagate along the opposite direction and re-emit to free space, which are detected in our experiment.

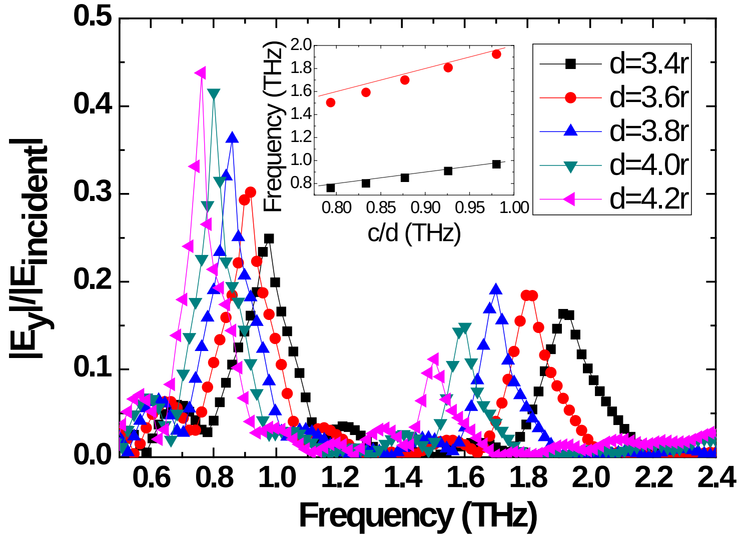

Fig. 5 Propagation spectra of the THz wave in arrays with different periods. The two lines in the inset represent *f*=*c/d* and *f*=2*c/d*, respectively.

In conclusion, we studied the propagation properties of terahertz waves in a one-dimensional metal arrays. It is shown that the metallic wire arrays can be used to transport terahertz waves at geometry dependent frequencies with low dispersion and at a speed very close to the speed of light in vacuum. This waveguide structure may be used in terahertz sensing and terahertz photonics. Further improvement of the inter-wire coupling efficiency may be achieved by changing the array structure and adding surrounding dielectric materials.

Acknowledgments

This work was supported by the National Natural Science Foundation of China under Grant Nos. 10834015 and 61077082.

References

1. M. Quinten, A. Leitner, J. R. Krenn, et. al.. "Electromagnetic energy transport via linear chains of silver nanoparticles". *Opt. Lett.* 23, 1331-1333 (1998)

2. J. R. Krenn, A. Dereux, J. C. Weeber, et. al.. "Squeezing the Optical Near-Field Zone by Plasmon Coupling of Metallic Nanoparticles". *Phys. Rev. Lett.* 82, 2590-2593 (1999)

3. Stefan A. Maier, Pieter G. Kik, Harry A. Atwater, et. al.. “Local detection of electromagnetic energy transport below the diffraction limit in metal nanoparticle plasmon waveguides”. *Nature Mater.* 2, 229-232 (2003)

4. Stefan A. Maier, Mark L. Brongersma, and Harry A. Atwater. “Electromagnetic energy transport along arrays of closely spaced metal rods as an analogue to plasmonic devices”. *Appl. Phys. Lett*. 78, 16-18 (2001)

5. J. B. Pendry, A. J. Holden, W. J. Stewart, et. al.. “Extremely Low Frequency Plasmons in Metallic Mesostructures”. *Phys. Rev. Lett.* 76, 4773-4776 (1996)

6. Kanglin Wang and Daniel M. Mittleman. “Metal wires for terahertz wave guiding”. *Nature*, 432, 376-379 (2004)

7. G. Shvets, S. Trendafilov, J. B. Pendry, et. al.. “Guiding, Focusing, and Sensing on the Subwavelength Scale Using Metallic Wire Arrays”. *Phys. Rev. Lett*. 99, 053903 (2007)

8. Wei Yan, Hua Chen, Yimin Sun, et. al.. “Spectral Responses by Chains of Subwavelength-Size Metallic Spheres in Terahertz (THz) Region”. *Terahertz Science and Technology* 2, 31-38 (2009).

9. A. Rice, Y. Jin, X. F. Ma, et. al.. “Terahertz optical rectification from <110> zinc-blende crystals”. *Appl. Phys. Lett*. 64, 1324-1326 (1994)

10. Paul C. M. Planken, Han-Kwang Nienhuys Huib J. Bakker, and Tom Wenckebach. “Measurement and calculation of the orientation dependence of terahertz pulse detection in ZnTe”. *J. Opt. Soc. Am. B*, 18, 313-317 (2001)

11. J. Homola, “Surface Plasmon Resonance Based Sensors”, Springer-Verlag, Berlin, (2006)